



# Differential dispersion and geometric calibration for BP/RP

---

prepared by: F. van Leeuwen  
affiliation : Institute of Astronomy  
approved by: CU5  
reference: GAIA-C5-TN-IOA-FVL-068-1  
issue: 1  
revision: 0  
date: 2011-08-16  
status: Issued

## **Abstract**

It will be possible to obtain a good calibration of the differential dispersion variations of the BP and RP photometers for Gaia early in the mission as part of the initialization of the geometric calibration. This note describes how this can be done.

## Document History

Issue	Revision	Date	Author	Comment
1	0	2011-08-16	FVL	release to Livelink
D	9	2011-08-16	SWB	Updated parameters for the dispersion polynomials
D	9	2011-02-24	FVL	Incorporated comments from CF and CJ
D	8	2011-02-08	FVL	Rewrote part of the introduction
D	7	2010-12-16	FVL	Further revised description of geometric calibration
D	6	2010-12-15	FVL	Revised part of the introduction and definitions
D	5	2010-12-10	FVL	Notation updates and general improvements
D	4	2010-12-09	FVL	Incorporated comments from Scott, restructured project files
D	3	2010-12-08	FVL	Incorporated comments from CJ
D	2	2010-11-26	FVL	Incorporated comments AB
D	1	2010-11-06	FVL	Changed title to agree with contents
D	0	2010-10-22	FVL	Creation

## Contents

<b>1</b>	<b>Introduction</b>	<b>4</b>
1.1	Objectives . . . . .	6
1.2	Applicable Documents . . . . .	6
1.3	References . . . . .	6
1.4	Definitions . . . . .	7
1.5	Acronyms . . . . .	10
<b>2</b>	<b>Description of a spectrum</b>	<b>10</b>
<b>3</b>	<b>The dispersion functions</b>	<b>11</b>
<b>4</b>	<b>Scaling the spectra</b>	<b>13</b>

<b>5</b>	<b>Aligning the spectra</b>	<b>15</b>
5.1	Cross-correlation fitting . . . . .	16
5.2	Binning and solving . . . . .	17
5.3	Curve fitting . . . . .	18
5.4	Fitting to the fitted curve . . . . .	19
5.5	Further iterations . . . . .	20
<b>6</b>	<b>Calibrating alignment and scaling</b>	<b>20</b>
<b>7</b>	<b>Setting the position of the reference sample</b>	<b>23</b>

## 1 Introduction

The processing of the BP/RP photometric data remains one of the most difficult elements of the Gaia data reductions. This is largely due to the combined effects the prism dispersion and instrument LSF have on the forming of an image from the spectral energy distribution (SED) of a source. As both the dispersion and the LSF are a function of the across-scan focal-plane coordinate ( $X_{\text{fpa}}$ ) of the image, it follows that images as observed at different across-scan positions cannot be related through exact transformations, complicating the definition of internally calibrated spectra. However, there are some initial calibrations one can do concerning the image stretching (dispersion variations) and positioning (geometric calibration) that can provide a common pseudo wavelength scale for all spectra, and thus make easier the comparisons between the sampled spectra obtained at different AC positions or FoVs. The common pseudo-wavelength scale allows for a direct comparison between responses (samples) obtained in spectra at different AC and AL positions and in different FoVs. The remaining differences between such “partially normalized” spectra are primarily due to the smearing effect of the LSF, which itself depends on AC-position and wavelength. They are of course also affected by local variations in the CCD responses.

The pseudo wavelength scale can also be used for accumulation and representation of the mean spectra. This scale is by definition relative, i.e. it can be defined through the position of a single reference point (reference pseudo wavelength) on, say, a grid of 60 samples, and a reference dispersion function relative to the reference point. Together these define the (relative) sample positions of the pseudo wavelengths and *vice-versa* in the mean spectrum. The pseudo wavelength scale for any spectrum as observed by the instrument can be related to the representation of the mean spectrum through identification of the reference point, which we will define as the Artificial Reference Sample (ARS), and a local adjustment (scaling) for the dispersion. The identification of the ARS position ( $\kappa_{\text{ARS}}$ ) for observed spectra of different types is obtained through the geometric calibration, which by definition identifies the position in an observed spectrum that corresponds with the effective wavelength of the ARS.

The geometric calibration can be described as a combination of two transformations. The first of these predicts the focal plane coordinates ( $X_{\text{fpa}}, Y_{\text{fpa}}$ ) of the observed source for a given time associated with the observations, for example the mean observation time for the 60 samples. This can simply be the default projection for the optical system as applied to the apparent source position at the mean time of observation. Together with the default positions of the CCDs and the focal length of the telescope, this translates into a pixel position at the chosen reference time. The second transformation defines what should be a small correction from this initial prediction to a final position applicable to the ARS. This is the geometric calibration we have to determine and apply in our reductions in order to relate spectra of different types and as observed at different focal plane positions to the same pseudo wavelength scale.

As will be shown in Section 3, the differential effects of the dispersion amount to a relative scaling of the sample widths and positions, and a similar effect on the responses. This scaling itself turns out to be a very simple function of the across-scan focal plane coordinate, reflecting the tilt of the prism. As long as the effects are described in focal plane coordinates, the small differences in beam shape between the two FoVs have a very minor effect on this. This follows from the principle-ray calculations on the optical design by Astrium.

The two differential effects described briefly above can be calibrated already very early in the mission, using selections of stars in one or more relatively narrow spectral ranges; how narrow is still to be found out from experiments. When doing the geometric calibration in a narrow spectral range, the alignment of the spectra does not involve the position of the ARS, but is done directly on the spectral responses. The position of  $\kappa_{\text{ARS}}$  can then be defined for the mean spectrum derived from those data. This can be done such that the difference between the mean and effective wavelength at  $\kappa_{\text{ARS}}$  show minimal differences over a wide range of spectral types (see further Section 7). With the definition of the ARS position, the dispersion variation and the geometric calibrations, BP/RP observation for any spectral type, and on any CCD, can be transformed to the same common pseudo wavelength scale.

There are a few differences with the approach used for a similar calibration in (JMC-003). The dispersion corrections across the focal plane, and between the two fields of view, are linked through a simple low-order polynomial; the effects of the LSF variations are seen as being of secondary importance in these calibrations; and the definition of a reference pseudo wavelength ( $\kappa_{\text{ARS}}$ ) is introduced to provide a link between the geometric calibration and a pseudo-wavelength scale. Furthermore the solutions are done by linear least squares over all CCDs together to provide a full internally consistent pseudo-wavelength scale for any spectrum as measured on any CCD. A linear least-squares solution is simpler and faster than the  $\chi^2$  minimization through maximum likelihood as used in (JMC-003), and provides in addition direct estimates of formal errors on the solved-for parameters. (JMC-003) does provide an insight into the suitability of sources of different spectral types for this type of calibrations.

The calibrations described here provide a means of ‘un-loading’ the  $a_{ij}$ -coefficients solutions (JMC-006), by removing the need to not only compensate for the LSF variations (and their interaction with the spectral features), but also having to correct for geometric offsets and dispersion differences. The compensation for, and interpretation of, geometric calibration and dispersion corrections as absorbed by the  $a_{ij}$ -coefficients is much less straightforward, in particular when trying to incorporate dependencies (constraints) on the AC coordinate of the observations for the dispersion variations. By removing this part of the dependencies from the  $a_{ij}$ -coefficients solutions, the actual coefficients become cleaner and easier to control and interpret.

In the context of absolute calibration of the dispersion the current approach provides a single reference between the external and internal calibrations, which is well defined in pseudo-wavelength scale.

## 1.1 Objectives

This note sets out to describe a method for deriving the differential and AC-dependent geometric and relative dispersion calibrations as applicable to the BP and RP photometers.

## 1.2 Applicable Documents

When applicable documents change a change may be required in this document. The applicable documents are listed here for clarity - the full reference is below in Sect. 1.3.

- FVL-001 CU5 Software Development Plan
- FVL-074 CU5 Software Requirements Specification, top level
- CF-012 Proposal for internal calibration of XP spectra

## 1.3 References

- [BAS-003], Bastian, U., 2007, *Reference systems, conventions and notations for Gaia*,  
GAIA-CA-SP-ARI-BAS-003,  
URL <http://www.rssd.esa.int/l1ink/livelihood/open/358698>
- [AB-009], Brown, A., 2007, *Photometry with dispersed images - overview of BP/RP data processing*,  
GAIA-C5-TN-LEI-AB-009,  
URL <http://www.rssd.esa.int/l1ink/livelihood/open/2329785>
- [JMC-003], Carrasco, J., Jordi, C., Fabricius, C., Figueras, F., Voss, H., 2007, *Chi-squared minimisation for wavelength calibration*,  
GAIA-C5-TN-UB-JMC-003,  
URL <http://gaia.esac.esa.int/dpacsvn/DPAC/CU5/docs/GAIA-C5-TN-UB-JMC-003/GAIA-C5-TN-UB-JMC-003.pdf>
- [JMC-006], Carrasco, J.M., Fabricius, C., Jordi, C., et al., 2009, *A simple calibration model for BP/RP spectra*,  
GAIA-C5-TN-UB-JMC-006,  
URL <http://www.rssd.esa.int/l1ink/livelihood/open/2892507>
- [CDO-001], Domingues, C., Rebordao, J., 2009, *Dispersion Analysis*,

GAIA-C2-TN-INET-CDO-001,

URL <http://www.rssd.esa.int/l1ink/liveliink/open/2860520>

[CF-012], Fabricius, C., Jordi, C., van Leeuwen, F., et al., 2009, *Proposal for internal calibration of XP spectra*,

GAIA-C5-TN-UB-CF-012,

URL <http://www.rssd.esa.int/l1ink/liveliink/open/2922510>

van Leeuwen, F., 2007, *Hipparcos, the New Reduction of the Raw Data*, Springer, Astrophysics and Space Science Library. Vol. 350 edn.

[LL-084], Lindegren, L., 2009, *Minimum-dimension LSF modelling*,

GAIA-C3-TN-LU-LL-084,

URL <http://www.rssd.esa.int/l1ink/liveliink/open/2915742>

[FVL-074], van Leeuwen, F., Richards, P., 2011, *CU5 top-level Software Requirement Specifications*,

GAIA-C5-SP-IOA-FVL-074,

URL <http://www.rssd.esa.int/l1ink/liveliink/open/3073983>

[FVL-001], van Leeuwen, F., Richards, P.J., 2010, *CU5 Software Development Plan*,

GAIA-C5-PL-IOA-FVL-001,

URL <http://www.rssd.esa.int/l1ink/liveliink/open/497754>

[HV-001], Voss, H., Jordi, C., Fabricius, C., et al., 2007, *AC flux loss analysis for AF and BP/RP*,

GAIA-C5-TN-UB-HV-001,

URL <http://www.rssd.esa.int/l1ink/liveliink/open/2746204>

## 1.4 Definitions

The effective spectrum  $\phi(\lambda)d\lambda$ , expressed in photons, is defined here as what is left of the actual spectral energy distribution (SED) of a source after passing through the Gaia optics, the photometric filters and the wavelength-dependent quantum efficiency of the CCD, i.e. the spectral response that would be obtained if we could deconvolve the observed spectra with the actual, wavelength-dependent, point-spread function (PSF). The effective spectrum thus defined is independent of the AC position of the observed spectrum, assuming that small variations in the individual CCD responses can be calibrated out.

The monochromatic PSF,  $P(\kappa - \kappa_0, \mu - \mu_0 | \lambda, \overline{Y_{\text{fpa}}}, X_{\text{fpa}}, \text{FoV})$ , describes the normalized response in the focal plane as produced by the telescope (indicated by FoV) for a given wavelength  $\lambda$  and position in the focal plane  $\overline{Y_{\text{fpa}}}, X_{\text{fpa}}$ , which are the coordinates in

the focal plane assembly as defined in (BAS-003), measured from the centre of CCD row 4. The responses are expressed for positions relative to a central position (see e.g. LL-084 on how this centre position may be defined) given by  $(\kappa_0, \mu_0)$ . In practise a PSF function may only be known as a ‘discrete’ function of  $\lambda$ , averaged over an interval  $d\lambda$ , rather than a continuous function of  $\lambda$ . The image shape is determined by the PSF applicable to the coordinates in the focal plane  $(\overline{Y_{\text{fpa}}}, X_{\text{fpa}})$  and the field of view (FoV). The image represents a PSF that is always integrated along-scan over (part of) the CCD, and therefore an average over  $Y_{\text{fpa}}$ , and also includes the effects of TDI smearing and sampling. This average depends on the gate activation, and represents an effective PSF that can in principle be derived from the observations in an absolute calibration of the spectral responses. The image shape is also affected by the local across-scan velocity of the FoV at the time of observation, which will cause smearing of the effective PSF in  $\mu$  over up to 4 CCD pixels in the across-scan direction.

The monochromatic line-spread function (LSF),  $L(\kappa - \kappa_0 | \lambda, \overline{Y_{\text{fpa}}}, \mu_i, \text{FoV})$ , is the PSF integrated over 12 across-scan pixels ( $\mu$ ) as centred by the on-board software on a window position  $\mu_i$  (which would normally be close to, but not the same as,  $\mu_0$ ). The LSF is therefore a function of  $\mu_i - \mu_0$ , though this is a minor effect in the context of the current calibrations (but not a minor effect when considering flux calibrations, see also HV-001). The resulting 1D image shape is in addition dependent on the local across-scan velocity  $\dot{\mu}$ , which affects the position difference  $\mu_i - \mu_0$  as a function of the integration time. The LSF is normalized such that

$$\int_{-\infty}^{\infty} L(\kappa - \kappa_0 | \lambda, \overline{Y_{\text{fpa}}}, \mu_0, \text{FoV}) d\kappa = 1. \quad (1)$$

The AC velocity  $\dot{\mu}$  for an observation is in first approximation a function of the rotation phase  $\Omega(t)$  of the satellite’s  $x$  axis in the SRS (BAS-003) (half-way between the two FoVs). This rotation phase is measured from the crossing of the scan circle with the great circle through the spin-axis position and the nominal direction of the Sun as seen from the satellite. The dependence reflects the displacement as a function of time of the spin axis in the celestial reference frame as it follows the nominal scanning law. The local variation of the AC velocity at an along-scan focal-plane position  $\overline{Y_{\text{fpa}}}$  is approximately given by

$$\dot{\mu} \simeq 170(\text{mas/s}) \sin(\Omega(t) \pm 0.5\gamma + \overline{Y_{\text{fpa}}}), \quad (2)$$

where  $\gamma$  is the basic angle between the two fields of view. The + sign refers to observations in the preceding FoV, the – sign to the following FoV, showing that generally there will be different AC velocities applicable to the two FoVs (see also van Leeuwen (2007)).

The dispersion function

$$\kappa = \kappa(\lambda - \lambda_0, X_{\text{fpa}}) \quad (3)$$

describes the relation between the wavelength  $\lambda$  and relative pixel positions  $\kappa$  that can be applied to an effective spectrum. The function  $\kappa$  returns a value of zero for  $\lambda = \lambda_0$ . Physically, the dispersion function is defined by the optical properties of the prism and the positioning of the prism relative to the FPA. The projection of the dispersed image on the focal plane depends on the distance of the prism from the focal plane. The relation between relative positions on the focal plane and wavelength of the incoming light should therefore in first approximation be independent of the FoV, which is confirmed by the principle-ray measurements by Astrium. The differences between the optical centres for the two fields of view has therefore no measurable influence the dispersion. The approximately linear scaling of the dispersion, which had been suggested before by Anthony Brown, as function of the  $X_{\text{fpa}}$  of the transit is given by:

$$\kappa(\lambda - \lambda_0, X_{\text{fpa}}) \simeq \kappa(\lambda - \lambda_0, 0) \cdot (1 + s(X_{\text{fpa}})), \quad (4)$$

The factor  $s$  can in first approximation be obtained from ground-based calibrations, and corrections to it are part of the calibration described in this note. The inverse of the dispersion function,  $\Lambda$ , is given by:

$$\Lambda(\kappa, X_{\text{fpa}}) = \lambda - \lambda_0. \quad (5)$$

The predicted focal plane position at the observation time for a measurement is obtained from the optical projection and satellite attitude, astrometric parameters for the observed source and various ephemerides. It is given in the along-scan direction as the position  $\kappa_f$  with respect to the extracted samples at observation time. Thus,  $\kappa_f$  is a focal plane position provisionally transformed to a CCD-readout position. In fact, not the actual values of  $\kappa_f$  is what we are interested in, but only differences. For this we can define a mean  $\overline{\kappa_f}$ , and preserve the differences

$$\Delta\kappa_f \equiv \kappa_f - \overline{\kappa_f} \quad (6)$$

for each observation. As we are not using the BP/RP data for astrometry, the exact definition of  $\overline{\kappa_f}$  is not critical, though, once set, its value should not be changed. To further assist the processing, these differences can be transformed to samples based on the focal length calibration by Astrium at the start of the mission. Considering that these are only small values, the conversion to samples doesn't require an extremely accurate focal length to be used. The reference time for calculating the focal plane position can be observation time for the transit. At first assignment the  $\Delta\kappa_f$  values will be distributed randomly within a range of about 4 to 6 samples. They will only become aligned once the spectra have been aligned. Alternatively, the spectra will become approximately aligned when aligning them on their  $\Delta\kappa_f$  values. The geometric calibration provides the information to go from this approximate to an accurate alignment. The geometric calibration will still be a function of  $X_{\text{fpa}}$ , with local offsets and orientation variations per CCD, as well as small, of order 0.01 pixel, systematic variations per stitch field on each CCD. The position of a spectrum in the focal plane will need to be identified

with a unique position in the spectrum, for which we use the artificial reference sample  $\kappa_{\text{ARS}}$  (see above). The transformation from  $\Delta\kappa_f$  to  $\kappa_{\text{ARS}}$  is referred to as the geometric calibration of the photometric instrument.

Together with the calibration of the differential effects of the dispersion function across the focal plane, the geometric calibration, as defined for the ARS, provides a unique relation between any observed sample position and a uniform set of pseudo wavelengths. This reference system is very close to that of the centre of CCD 4 in either BP or RP.

## 1.5 Acronyms

The following is a complete list of acronyms used in this document. The following table has been generated from the on-line Gaia acronym list:

Acronym	Description
AC	ACross scan
AL	ALong scan
ARS	Artificial Reference Sample
BP	Blue Photometer
CCD	Charge-Coupled Device
CF	Conversion Factor [e- per ADU]
FPA	Focal Plane Assembly (Focal Plane Array)
FoV	Field of View (also denoted FOV)
GOG	Gaia Object Generator
LSF	Line Spread Function
PSF	Point Spread Function
RP	Red Photometer
SED	Spectral Energy Distribution
SRS	Software Requirements Specification
TDI	Time-Delayed Integration (CCD)
XP	Shortcut for BP and/or RP

## 2 Description of a spectrum

The dispersed image  $r(\kappa)$  (giving the flux per sample at sample position  $\kappa$ ) for a (continuous) pixel position  $\kappa$  as created by one of the photometers from the **effective spectrum**  $\phi(\lambda)d\lambda$  as defined above in Section 1.4 (and not starting from the SED as is

done in, for example, AB-009) is given by

$$r(\kappa) = \frac{\int_{\kappa-D\kappa}^{\kappa+D\kappa} L(\kappa_c - \kappa|\Lambda(\kappa_c)) \left[ \phi(\Lambda(\kappa_c) - \lambda_0) \frac{\partial d\lambda}{\partial \kappa_c} \right] d\kappa_c}{\int_{\kappa-D\kappa}^{\kappa+D\kappa} L(\kappa_c - \kappa|\Lambda(\kappa_c)) d\kappa_c}, \quad (7)$$

using the inverse dispersion function of Eq. 5 to describe the LSF and effective spectrum in relative pixel positions. It is assumed here that the effective spectrum is already scaled to provide the relevant flux for a star. The integration limits should in principle be infinite, but in reality are limited to a range of  $\pm D\kappa$ , depending on the relevant contributions from the LSF.

The “image” as represented by Eq. 7 is continuous rather than the actual image, which is sampled. However, the smearing caused by the sampling can be included in the LSF function  $L$ , in which case the predicted spectrum  $R$  at sample positions  $k$  is simply obtained from the responses of  $r$  as defined in Eq. 7 at the required sample positions. For this is needed the position of  $r$  with respect to the recorded string of 60 samples. This is defined by the predicted focal plane position for the end of sample 30, and the geometric calibration evaluated at the AC position  $X_{\text{fpa}}$ , to obtain the position  $\kappa_{\text{ARS}}$  within the 60 samples of the observation record. Assuming that  $\kappa$  is simply a linear function of  $k$ , the responses at all pixel positions can be read out from  $r$ , to create a predicted sampled spectrum  $R(k)$  associated with a reference position  $\kappa_{\text{ARS}}$ .

### 3 The dispersion functions

The Gaia parameter data base provides a modelling of the dispersion functions in BP and RP, and for the two fields of view, as two 3D arrays:

```
:Satellite:BP:Spectrum_DispersionFunction_Fitted
:Satellite:RP:Spectrum_DispersionFunction_Fitted
```

These functions were derived by Astrium through chief-ray analysis through the optical system. They provide the dispersion functions at the centres of the 7 CCDs for BP and RP. Expressed as functions of the inverse wavelength, they provide relative focal plane positions in mm relative to the position associated with a reference wavelength, 440 nm in BP and 800 nm in RP. The analysis of the dispersion functions presented here creates a very much simpler, though still sufficiently accurate, 2D representation than has been presented by CDO-001. Simple differential relations are beneficial when trying to analyse the data, as this limits the degrees of freedom and improves solution stability.

A comparison between the functions for different CCDs (thus, at different AC positions), shows that the functions for the same channel and FoV are to a high degree related

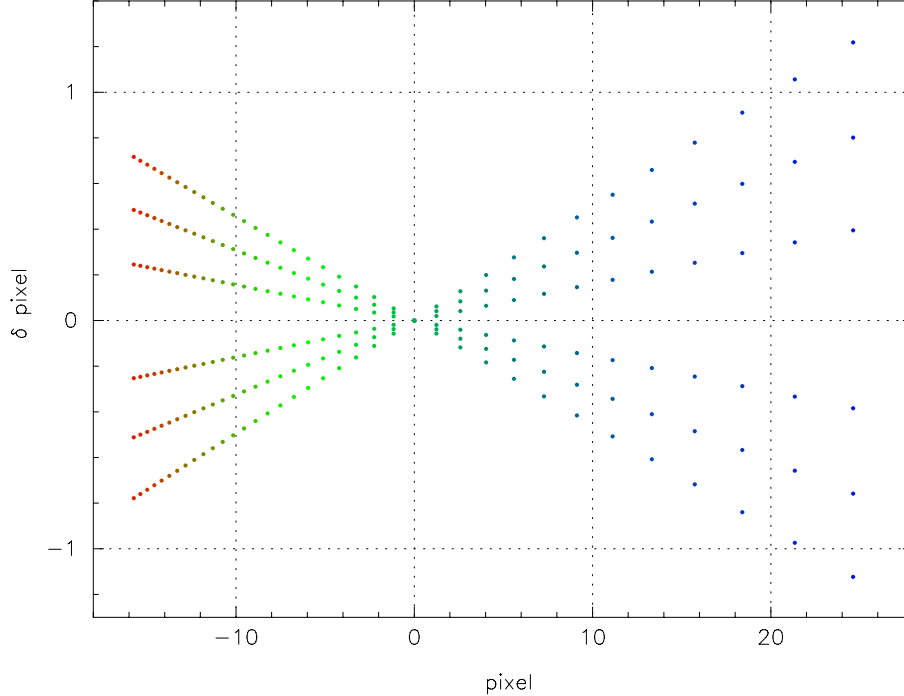


FIGURE 1: Pixel position offsets, with respect to CCD-4, as measured at the same wavelengths, for the BP dispersion curves in telescope 1. The wavelength range covers 320 nm to 690 nm, the reference wavelength is at 440 nm. The colours of the dots are an indication of the associated wavelength.

through a linear scaling (Fig. 1). In addition, the differential relations are as good as identical between the two fields of view. In the Astrium model the dispersion function for each CCD is accurately expressed as a 3rd order polynomial of the inverse wavelength  $\nu = 1/\lambda$  (with  $\lambda$  in nm) in BP, and similarly a 4th order polynomial in RP:

$$\kappa(\nu) = \sum_{i=0}^{i=3} a_i \cdot \nu^i. \quad (8)$$

This relation is defined such that at  $\nu = \nu_0$  (the reference wavelength) the function in Eq. 8 returns zero. If we start our analysis at the centre ( $X_{\text{fpa}} = 0$ ) of the focal plane, halfway CCD4, then the dispersion at any other AC position can be expressed as:

$$\kappa(\nu|X_{\text{fpa}}) = [1 + s(X_{\text{fpa}})] \cdot \kappa(\nu|X_{\text{fpa}} = 0). \quad (9)$$

For the function  $s(X_{\text{fpa}})$  a simple second-order polynomial in  $X_{\text{fpa}}$  is sufficient to represent the  $X_{\text{fpa}}$  dependencies for both fields of view at the same time. Table 2 shows as an example the evaluation for the RP channel in telescope 1. If we give the  $X_{\text{fpa}}$  position of the centre of CCD1 as  $-3$ , of CCD4 as  $0$ , and CCD7 as  $+3$ , then the following relation is found for  $s$ :

$$s_{\text{RP}}(X_{\text{fpa}}) = -0.0149 \cdot X_{\text{fpa}} + 0.001221 \cdot X_{\text{fpa}}^2. \quad (10)$$

CCD	Range	Ratio	$s$	$\tilde{s}$
1	33.9149	1.0554	0.0554	0.05558
2	33.2435	1.0345	0.0345	0.03461
3	32.6497	1.0161	0.0160	0.01609
4	32.1339	1.0000	0.0000	0.00000
5	31.6967	0.9864	-0.0136	-0.01364
6	31.3381	0.9752	-0.0248	-0.02485
7	31.0586	0.9665	-0.0335	-0.03361

TABLE 2: Relations between the dispersion functions for the centres of the 7 RP CCDs. Column 1: CCD; 2: Pixel range between  $\lambda = 630$  nm and 1050 nm; 3: Range ratio with respect to CCD4; 5: value for the function  $s$  as in Eq. 9; 6: fitted value for  $s$ .

Residuals with respect to this fit are also shown in Table 2, and are at the numerical round-off level, well below what is still significant for the analysis of the BP/RP data. A similar relation is found for the BP CCDs:

$$s_{\text{BP}}(X_{\text{fpa}}) = -0.0161 \cdot X_{\text{fpa}} + 0.000220 \cdot X_{\text{fpa}}^2. \quad (11)$$

In the current application we are only interested in the differential effects of the dispersion, for which Eq. 10 and 11 provide all the necessary information. These relations are independent of the units in which the function  $\kappa(\nu)$  is expressed. It is in addition worth noting that the pixel positions at the limits of the wavelength coverage for the images as produced by the two FoVs differ by no more than a few thousandth of a pixel either side. In that sense it is also possible to compare images from the different FoVs for an initial differential dispersion calibration.

## 4 Scaling the spectra

Scaling of the observed spectra attempts to remove the first-order effects of the dispersion variation over the focal plane. It effectively re-aligns the samples of spectra taken at different  $X_{\text{fpa}}$  positions to uniform pseudo-wavelength positions. The actual values of the wavelengths are not important at this stage of the analysis. The scaling has to take into account not only the positional displacement, but also the effective width of the samples as expressed in the pseudo wavelength scale (or, more precisely, do

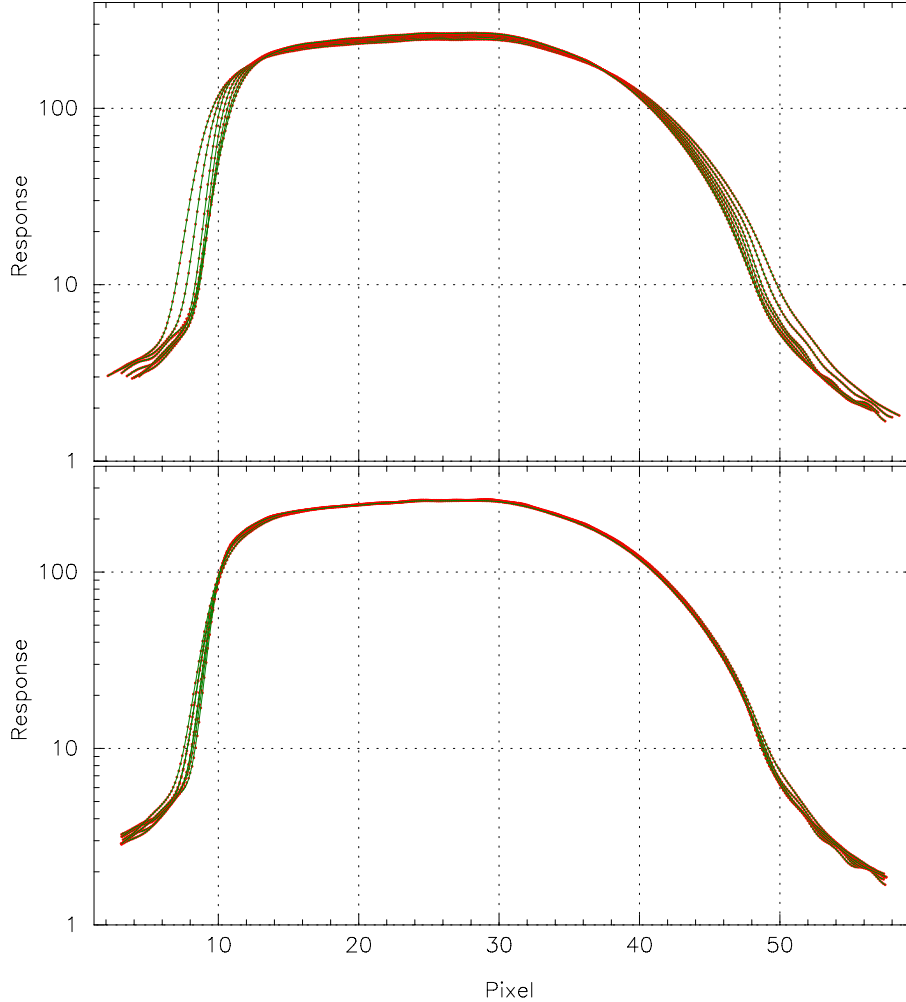


FIGURE 2: Normalization of over-sampled and noise-free simulated spectra in RP, for a ( $T=7000$ ,  $\log g = 4.5$ ) star. Top: spectra as observed, aligned to a single reference pseudo wavelength. Bottom: the same spectra, re-scaled according to the differential dispersion relations.

an integration of the response over the sample width, CF-012). This amounts to keeping the “surface area” for each sample constant, so when the observed sample response is projected on a narrower reference sample response, the response will in first approximation be increased by the same factor by which the width of the sample was decreased:

$$R'(\kappa) = \frac{1}{1 + s(X_{\text{fpa}})} R(\kappa \cdot (1 + s(X_{\text{fpa}}))), \quad (12)$$

where  $\kappa$  is used instead of  $k$  to indicate that the spectra have been aligned in along-scan direction on a continuous pixel scale. The function  $s$  is the same as defined above in Eq. 9.

Scaling of the spectra is done relative to the position of  $\kappa_{\text{ARS}}$ , and therefore involves a definition of the  $\kappa_{\text{ARS}}$  position in the spectrum. On the other hand, determination of  $\kappa_{\text{ARS}}$  is difficult when scaling has not been done. However, if we can assume the scaling (the differential dispersion) to be quite accurately known at any time (starting from ground-based specifications), then the further scaling correction is going to be very small, and will hardly affect the determination of  $\kappa_{\text{ARS}}$ . An example of this scaling, using GOG data, is shown in Fig. 2.

## 5 Aligning the spectra

Aligning of spectra of the same type is used to establish the geometric calibration for the BP and RP detectors. This geometric calibration establishes a relation between predicted focal plane position at the time of observation ( $\Delta\kappa_f$ ) and a reference sample position  $\kappa_{\text{ARS}}$  in the spectrum. The geometric calibration is established based on one or more narrow groups of spectral types, thus stars with spectral images that are very similar in shape, and only differ in the total flux. The spectra may also need to come from a restricted range in magnitude, to limit the mixing of reddening and temperature effects in the spectra.

In the following, a calibration unit (CalU) represents a single combination of CCD, FoV and gate. The procedure is as follows:

1. Collect for a time interval all observed spectra (corrected for background contributions, but keep a record of the original photon counts for error assessments) within one or more narrow spectral ranges; the width in spectral range that can be used is still uncertain, and likely to be itself function of spectral type;
2. Normalize the flux and errors according to the integrated counts, this is the first approximation of the total flux;
3. Separate the thus prepared spectra per CalU, to get relatively homogeneous samples in LSF;
4. Per CalU, select an arbitrary reference observation (spectrum) from the above selection, preferably bright and close to the centre of the CCD in AC direction (Sect. 5.1); this only serves as an initial reference to start the iterative fitting procedures;
5. Determine  $\Delta\kappa_f$  for each observation as described in Section 1, this will serve as input for the differential geometric calibration for the CalU; note that  $\overline{\kappa}_f$  has to have the same value for all CalUs;

6. Through cross-correlation, align all other spectra obtained in each CalU to the selected reference spectrum;
7. Based on the correlation statistics, eliminate poorly fitting (wrongly selected) data;
8. Collect per CalU the aligned data in bins at some fraction of the sample width (suggest 1/4); this includes information on the formal errors
9. Determine mean normalized responses and errors per bin; normalized responses all have the same integrated response over the background- and CTI-corrected sampled data;
10. Fit the binned data for CCD4 in one of the FoVs, and no gate, with a spline function, re-normalize the response based on the integral of the fitted function;
11. Re-align in position and flux all selected data per CalU with the fitted spline function (see below);
12. Collect again in bins, this time correcting for the differential dispersion variations across each CalU, determine means, and fit;
13. At this stage the AC resolution of the geometric calibration may be increased, with possibly one or two points per stitch field;
14. Repeat the above processes until corrections to normalization factors for the fluxes and the positional corrections become negligible;
15. Correct the total shift corrections as determined in the fitting described above for  $\Delta\kappa_f$ , collect the differences as a function of  $X_{\text{fpa}}$ ; this is the geometric calibration, which should be added to  $\Delta\kappa_f$  to obtain the position of  $\kappa_{\text{ARS}}$ .

## 5.1 Cross-correlation fitting

The cross-correlation process (points 6 and 7 above) is only required for initialization of the geometric calibration. It is carried out over the range of the observed spectrum that falls within the relevant instrument wavelength range. For RP this is approximately 630 to 1060 nm (38 to 42 pixels wide), for BP 320 to 690 nm (39 to 42 pixels wide). Spectra are collected in macro-samples, covering 4 actual samples, in a fixed pattern, i.e. start times of macro-samples are all synchronized. Thus, there is a variation of at least 4 samples for the positioning of a spectrum within the 60 samples received in an observation. Further variation in the positioning can be expected based on errors in the on-board predicted position of the spectrum.

The cross-correlation process is carried out per CCD, and uses arbitrary spectra as references, one per CCD and per FoV. The reference spectra should be relatively bright (but not saturated) and observed close to the AC centre of the CCD.

For the cross-correlation the 52 central samples (counting from zero, numbered from 4 to 55) of the reference spectrum, given by  $R(k)$ , are available. For each spectrum to be cross correlated with the reference spectrum, given by  $G(k)$ , the 40 central samples (numbered from 10 to 49) are used. The cross-correlation values  $X(j)$  are given by:

$$X(j) = \frac{\sum_{k=10}^{49} R(k+j) \cdot G(k)}{\sqrt{\sum_{k=10}^{49} R(k+j)^2 \sum_{k=10}^{49} G(k)^2}}. \quad (13)$$

The function  $X(j)$  is evaluated for  $-6 \leq j \leq 6$ . It is possible to reduce this range considerably by obtaining a first rough estimate of the “centering” of the spectrum within the 60 counts. This could be done, for example, by calculating the weighted mean position of the full range of the accumulated counts:

$$\langle k \rangle = \frac{\sum_{k=0}^{59} k \cdot G(k)}{\sum_{k=0}^{59} G(k)}. \quad (14)$$

Assuming that this returns, within a narrow range of spectra, approximately the same sample position with respect to the spectral image independent of the position of that image on the 60 samples, the differences between the mean positions for the reference and target spectra will provide the first estimate of the position of the maximum in the cross correlation. This then would provide a smaller set of target values for  $j$  to apply in evaluating  $X(j)$ .

The final step in the cross-correlation is the determination of the interpolated maximum in the distribution of the values found for  $X(j)$ . This is found by fitting the three (neighbouring) highest values of  $X(j)$  with a second-order polynomial in the position  $j$ . If  $X(j_0)$  is the highest value found in the cross-correlation, then this concerns the values from  $X(j_0 - 1)$  to  $X(j_0 + 1)$ , and the position of the maximum is found through:

$$j_{\max} = j_0 + \frac{X(j_0 - 1) - X(j_0 + 1)}{2X(j_0 - 1) + 2X(j_0 + 1) - 4X(j_0)} \quad (15)$$

From this it follows that the correlation between the spectrum  $G$  and the reference spectrum  $R(i)$  is highest when the pixel numbers are shifted by  $-j_{\max}$ , i.e. generally a non-integer number of pixels. This offset per observation should be preserved, as it is needed again as part of the first guess offset in the next step of the fitting (Section 5.4).

## 5.2 Binning and solving

For the binning and subsequent fitting (points 8 and 9) the way the sub-sample positions are defined is such, that the start of sample 0 is equivalent to position -0.5, the end of

sample 0 to position 0.5, and the end of sample 59 is position 59.5. Thus, initially the positions for the 60 samples are given as  $i$ , with  $i$  going from 0 to 59 (it could be considered too to accumulate for a wider range of samples to gain some insight in the extreme wings, though the data coverage will then be much reduced). If we now subdivide the samples into an odd number of bins then the samples of the reference spectra will fall in the central bin within a sample. Given  $n$  bins per sample, the bin number  $b$  assigned to a sample is given by the integer part of the shifted sample position:

$$b = \lfloor n \cdot (k + 0.5 - j_{\max}) \rfloor. \quad (16)$$

For the reference spectrum  $j_{\max} = 0$ . Data are only collected for bin numbers from 0 to  $60 \cdot n - 1$ .

The data collected per bin are the following:

$$\begin{aligned} S_1 &= \sum_j w_j \\ S_2 &= \sum_j w_j \cdot r_j \\ S_3 &= \sum_j w_j \cdot r_j^2 \\ S_4 &= \sum_j 1 \end{aligned} \quad (17)$$

where  $w_j = 1/\sigma_j^2$  is the weight for the normalized response  $r_j$  (as in item 3 in Section 5). This gives per bin the following results:

$$\begin{aligned} \langle r \rangle &= S_2/S_1 \\ \text{St.dev.} &= \sqrt{(S_3 - S_2^2/S_1)/(S_4 - 1)} \\ \sigma\langle r \rangle &= \text{St.dev.}/\sqrt{S_1} \end{aligned} \quad (18)$$

The pairs  $\langle r \rangle, \sigma\langle r \rangle$  per bin form the input to the next stage, curve fitting.

### 5.3 Curve fitting

The fitting of the data (point 10) primarily aims at providing a continuous reference curve for further alignment and scaling of the individual spectra. For the fitting can be used Householder splines routines as available through GaiaTools. The fit can be made over all available bins. The adjustment of the number and position of the nodes has to be decided on the remaining unit-weight standard deviation following the fit. In general, the spread of nodes can probably be less dense in the wings and more dense

in the core of the signal. Typical spread of nodes should reflect the scale-length of the variations in a spectrum, which is set by the width of the LSF, typically about 2 samples. Whatever way of fitting the data is used, it is assumed here that this produces a continuous function  $F(\kappa)$ , with a continuous derivative, representing the accumulated data. This spectrum can be “aligned” with an expected position through comparison with a simulated spectrum. This alignment, given by  $j_r$ , is not critical in any sense, it only ensures that the position of the curve with respect to the sampling positions is more or less where it would normally be found on average in the actual data. It results in the value of  $F(0.0)$  to be the predicted normalized response for sample 0. The alignment shift as applied should be preserved, as it provides part of the initial offset corrections used in the next stage of the fitting. A normalization of the area under the fitted curve, but covering only bins used in the fitting, should also be done. This normalization should not change much from the previous one, which was based on the reference spectrum, but helps to more accurately align data from different CCDs at a later stage.

## 5.4 Fitting to the fitted curve

By shifting for each observation the sampling positions by  $j_r$  and  $j_{\max}$  as defined in Eq. 15, the observed spectrum will be almost exactly aligned already with the fitted function  $F(\kappa)$ . At this stage we have to apply the small correction for the differential dispersion variation, over the AC range of each CCD, to the spectra (Eq. 12), which leads to corrections of up to 0.5 sample-positions either side of the useful part of the spectrum. This correction could not be done in the cross-correlation described above, as that method requires identical sampling for both inputs. In this next fitting step that is no longer a requirement, and samples can effectively be anywhere. The assumption is that the mean spectrum we obtained per CCD is closest to that at the mean AC position applying to transits for that CCD. The small scaling corrections to account for the dispersion gradient across a CCD should therefore bring each observation closer to the mean spectrum determined before.

The fine-tuning of the position and scaling of the spectra (points 10 and 11) follows from a comparison between the observed normalized counts and the predicted responses function  $F(\kappa)$  at the (transformed) sample positions. The fine tuning effectively adjusts the profile of  $F(\kappa)$  to the observations, then adjusts the observations and repeat the fitting until the adjustments become small with respect to the accuracies of the determinations. If by  $G'(\kappa)$  we denote the observed spectrum adjusted for the sample positions in shift and scale such as to fit the representation of  $F(\kappa)$ , then:

$$G'(\kappa) - F(\kappa) = dI \cdot F(\kappa) + \frac{\partial F(\kappa)}{\partial \kappa} d\kappa, \quad (19)$$

the solution of which by least squares leads to the following corrections for the observed

signal:

$$\begin{aligned} G''(\kappa') &= (1 - dI) \cdot G'(\kappa), \\ \kappa' &= \kappa - d\kappa, \\ I'' &= (1 - dI) \cdot I', \end{aligned} \tag{20}$$

where  $I'$  is the original total flux estimate for the transit. The weights applied in the least squares solution are set by the errors on the observed signal, scaled in the same way as the signal. The least squares solution provides formal errors on the two parameters,  $dI$  and  $d\kappa$ , which are used as criterion for the convergence of the solution.

A comparison between the recovered total flux and the formal error on  $d\kappa$  provides a reliable check on data quality and calibration limitations. Ideally we expect the following relation for these errors:

$$\sigma_{d\kappa} \approx \sqrt{n \cdot I + \sigma_c^2}, \tag{21}$$

where  $n$  is a normalization factor, and  $\sigma_c$  is the unresolved calibration noise.

## 5.5 Further iterations

Starting from the corrected observations as described by Eq. 19, and after eliminating any poor-fitting data, the remaining data are again collected in bins to obtain a new approximation for the profile  $F(\kappa)$ . An integrated flux correction can be obtained as a final correction. Then all data are again re-fitted, started with the corrected versions from the previous iteration cycle. However, the differential dispersion scaling should not be applied again, as this is already included in the corrected data. It is expected that in the second iteration step the calibration noise  $\sigma_c$  reduces, while also the variances on the binned data should reduce slightly. These observations can be used to determine a convergence of the iterations.

## 6 Calibrating alignment and scaling

The processes described above are carried out per CCD and FoV. The next step is to do a check on the assumed dependence of the dispersion function on the AC position, for which the indication is that this is a simple second-order dependency (see Section 3). The question is to what extent we can recover this relation in the presence of LSF functions that also contain an AC-coordinate dependence. The indication that the dispersion functions are nearly identical for the two fields of view can help here by diffusing correlations with the effects of LSF variations. The scaling for dispersion variations was given by Eq. 12 above. The default relation is applied to the data as

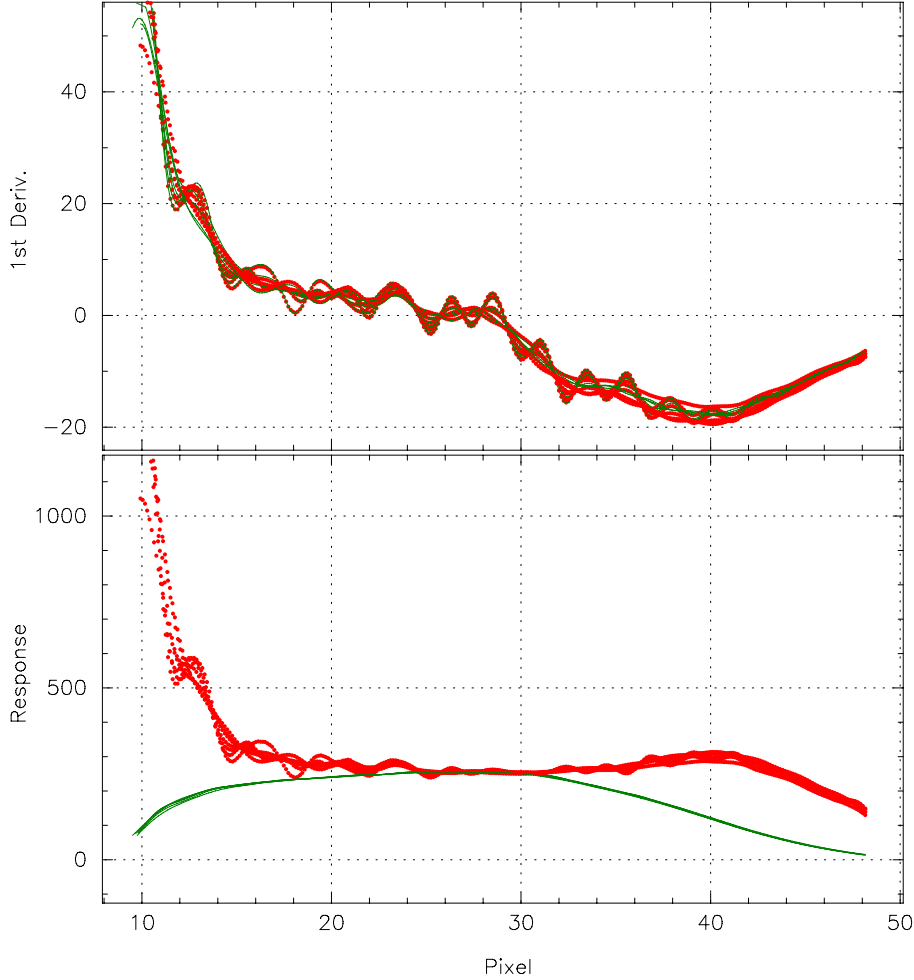


FIGURE 3: The coefficients  $\vartheta(\kappa)$  (top) and  $\varphi(\kappa)$  (bottom) for a 7000 K star in the RP channel, for all 7 CCDs.

collected for the 7 CCDs, reducing the dispersion for all to coincide with the dispersion on CCD4. It is expected that only very small corrections may need to be applied to account for the actual in-flight configuration parameters:

$$\left(\frac{1}{1 + \delta s}\right) F_a'(\kappa(1 + \delta s) + \kappa_a) = F_4(\kappa), \quad (22)$$

where  $F_a'$  is the response function at CCD  $a$ , corrected to CCD4 using the Astrium dispersion calibration as shown in Section 4,  $\delta s$  is the small adjustment to the assumed scaling from CCD  $a$  to CCD4, and  $\kappa_a$  is a correction for the positional offset in the definition of  $F_a$  with respect to the definition of  $F_4$  which occurs because of their independent determinations. However, as the same definition has been used for positioning the spectra in the different CCDs, the values of  $\kappa_a$  are expected to be small,

at the level of a fraction of a pixel only. That then leads to the following approximation:

$$F_a(\kappa)' - \delta s \left[ F_a(\kappa)' - \kappa \frac{\partial F_a(\kappa)'}{\partial \kappa} \right] + \kappa_a \frac{\partial F_a(\kappa)'}{\partial \kappa} = F_4(\kappa). \quad (23)$$

For each spectrum  $F_a'$  the data points used in the construction of the spectrum  $F_a$ , but after transformation to  $F_a'$  can be used rather than the fitted curve. The coverage in pixels should only include the effective wavelength coverage of the instrument, outside this range the response is fully LSF dominated. For  $F_4$  the continuous spline fit can be used.

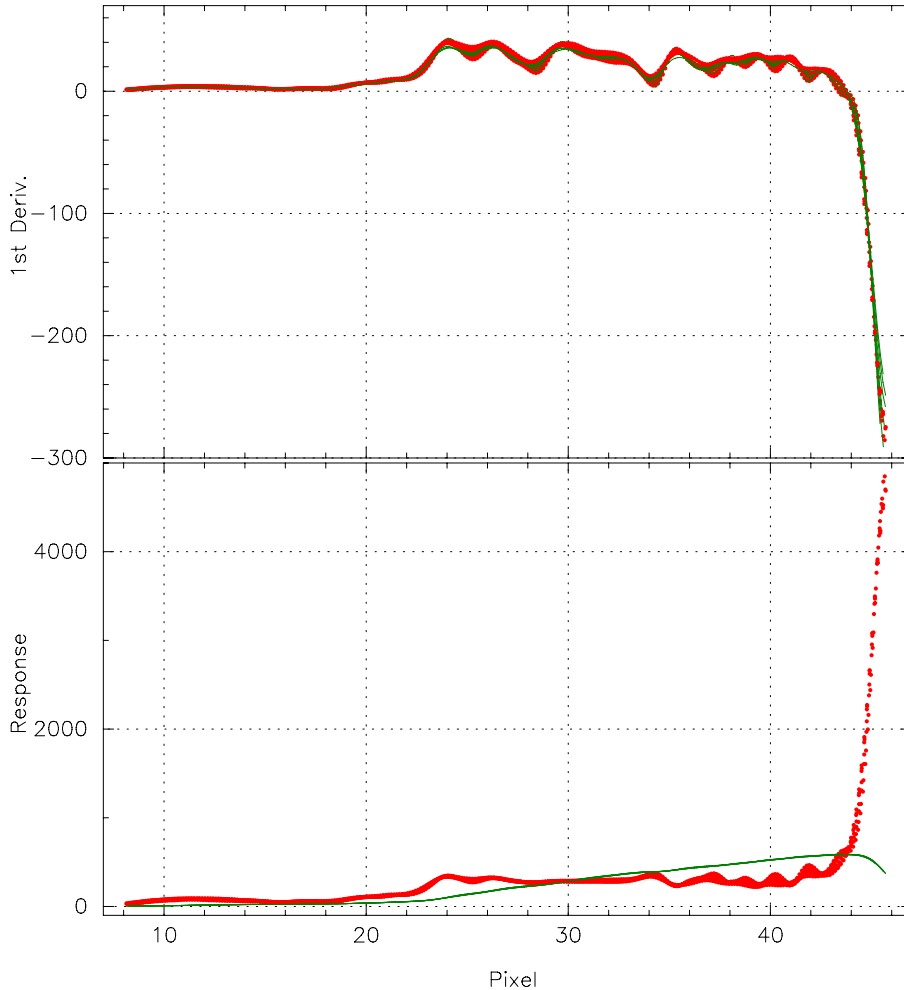


FIGURE 4: The coefficients  $\vartheta(\kappa)$  (top) and  $\varphi(\kappa)$  (bottom) for a 7000 K star in the BP channel, for all 7 CCDs.

The data from different CCDs and the two FoVs can be combined in one solution, where  $\delta s$  is represented as a second order polynomial in the AC position of the CCD relative to CCD4. The observation per bin, CCD and FoV is as follows:

$$(\delta s_0 \cdot X_{\text{fpa}} + \delta s_1 \cdot X_{\text{fpa}}^2) \varphi(\kappa) + x_a \vartheta(\kappa) = F_4(\kappa) - F_a(\kappa)' \quad (24)$$

The functions  $\varphi(\kappa) = \left[ F_a(\kappa)' - \kappa \frac{\partial F_a(\kappa)'}{\partial \kappa} \right]$  and  $\vartheta(\kappa) = \frac{\partial F_a(\kappa)'}{\partial \kappa}$  are shown for a 7000 K star in the RP channel in Fig. 3 and the BP channel in Fig. 4. Although showing similar features, they are essentially orthogonal and have only a small secondary dependence on the LSF, thus allowing in principle for a dispersion correction and the alignment of the spectra on the different CCDs to be solved in one solution for all CCDs and both fields of view, ensuring a geometric calibration that is fully consistent for all observations, and very good calibration of the dispersion function.

## 7 Setting the position of the reference sample

With the spectra aligned and scaled on all CCDs and for both FoVs, the position of the artificial reference sample ( $\kappa_{\text{ARS}}$ ) can be set as a reference point for the calibrations. To reconstruct the spectra in their original position on CCDs other than CCD4, the scaling, as defined through the Astrium dispersion determination and our own final in-flight corrections, can now be applied with respect to the position of  $\kappa_{\text{ARS}}$ , so that on all CCDs  $\kappa_{\text{ARS}}$  defines the same position in the spectrum. The  $\kappa_{\text{ARS}}$  position applies strictly to an effective wavelength, i.e. to the weighted response over the width of a sample. However, by defining the position of  $\kappa_{\text{ARS}}$  to a region of the spectrum where the curvature is generally very small, this secondary effect will be much reduced.

With these two differential calibrations in place, the ‘pre-processing’ of the BP/RP spectral data before submission to the  $a$ -coefficients, is now as follows:

- Determine the focal plane position as predicted for the end-time of sample 30, i.e. exactly halfway the 60 samples of the observation, correct for the reference position  $\overline{\kappa}_f$  to obtain  $\Delta\kappa_f$ ;
- Add to  $\Delta\kappa_f$  the geometric calibration according to the  $X_{\text{fpa}}$  position of the transit; a correction could be applied for the local AC scan velocity to obtain the relevant position at mid-time of the observation; this defines the position of  $\kappa_{\text{ARS}}$  in the observation;
- Apply the differential dispersion correction, again according to the  $X_{\text{fpa}}$  coordinate of the transit; this defines the uniform pseudo wavelength for each sample.

For every observed sample we thus obtain ‘corrected’ positions and responses, which are all on the same pseudo wavelength scale and response, independent of where on the focal plane they were obtained. The remaining differences between the transformed spectra come from the variations in LSF and the interaction between the LSF variations and the spectral features in the effective spectrum. Generally, the stronger those spectral

features are, the more sensitive this interaction becomes. As a result, the  $a$ -coefficients can only compensate partly for the LSF differences.

## Acknowledgements

Inputs to earlier versions of this note from Claus Fabricius, Carme Jordi, Anthony Brown, Scott Brown, Dafydd Evans and Francesca De Angeli were much appreciated.